

Densification, microstructure and properties of electroconductive Si_3N_4 –TaN composites.

Part I: Densification and microstructure

Vitaly Ya. Petrovsky^a, Zbigniew S. Rak^{b,*}

^a*Institute for Problems of Material Science Ukrainian Academy of Science, 3, Krzhyzhanovsky Str., 03142 Kiev, Ukraine*

^b*Netherlands Energy Research Foundation ECN, Westerduinweg 3, 1755 ZG Petten, The Netherlands*

Received 22 April 1999; received in revised form 20 June 2000; accepted 8 July 2000

Abstract

Dense Si_3N_4 –TaN composites with the TaN phase in the range of 5–50 vol.% were produced by a hot pressing technique in reducing (CO) and neutral (N_2) atmospheres. Two types of ceramic items in the form of three dimensional components and functionally graded material were evaluated. The influence of densification parameters, amount and grain size of TaN particles and geometry of the functional zone on the microstructure, mechanical properties and electrical resistivity was investigated. It was found that the use of a coarse, non stoichiometric TaN powder as a second component of the composite, combined with a reducing atmosphere in the sintering process, resulted in the formation of a chain type network of the electroconductive phase. The formation of new phases such as SiC, Ta_5Si_3 , $\text{TaC}_{0.5}\text{Si}$ in the composite body were also recorded. A quite different microstructure was observed when the composite material was sintered in a nitrogen atmosphere or a fine TaN powder was used. The latter composites were characterised by a ring-type network of the conductive phase in the insulating matrix. The conducting particles formed the monolithic and isometric structure of the conductive clusters. Apart from the Si_3N_4 and TaN such new phases as $\text{Ta}_5\text{Si}_3\text{N}_7$ and TaSi_2 were identified in the sintered composite material. © 2001 Elsevier Science Ltd. All rights reserved.

Keywords: Composites; Hot pressing; Microstructure-final; Si_3N_4 –TaN; Sintering

1. Introduction

Advanced structural ceramics based on nitrides and carbides are well known candidates for replacement of conventional metal parts in gasoline and diesel engines and gas turbines. They can also be used as bearings and wear parts.^{1–3} They have been widely studied in order to improve their mechanical, electrical and thermal properties. Recently ceramic matrix composite (CMC) materials with controlled electrical conductivity have been replacing metal parts in special electrical and electronic devices, which not only increases the performance of these components but also the range of applications for advanced ceramics. Electroconductive composite materials are also widely used in industrial applications as resistors, sensors and transducers, e.g. thermistors or incandescent bodies in electrical heaters. When the

electroconductive composite consists of the insulator as a matrix and the conductor as a secondary phase (filler), then the overall electrical properties of the electroconductive composite are governed by the percolation behaviour through the formation of a continuous network of conductive particles throughout the insulating matrix. It has been observed that in the electroconductive composite with a certain volume fraction of the conductor X_m , there exists a threshold conductor volume fraction, X_c , above which the electrical conduction takes place through the composite. The electrical resistivity of the electroconductive composite strongly depends not only on the X_m , but also on the X_c , which in turn strongly relies on the microstructure of the composites.^{4,5} In general, the electroconductive composites are a typical case of two-phase microcracking ceramics.^{6,7} The composites are formed very often from low-expansion phases such as the ceramic materials and high-expansion phases like intermetallics. Agglomerates larger than a certain critical size present in the conductive composite are a source of flaws which, in turn,

* Corresponding author.

E-mail address: rak@ecn.nl (Z.S. Rak).

Nomenclature			
CMC	ceramic matrix composite	D	size of ellipsoid (diameter) in the direction perpendicular to the current flow
FGM(C)	functionally graded material (composite)	ρ_{20}	resistivity at room temperature (20°C)
TaN	tantalum nitride	ρ_T	resistivity at “T” temperature
SiC	silicon carbide	ρ_P	electrical resistivity of the CMC material
Si ₃ N ₄	silicon nitride	ρ_{ins}^d	electrical resistivity of the insulator phase
BN	boron nitride	ρ_m	electrical resistivity of the conductor phase
HP	hot pressing	z_m	effective coordination number of the conductive particles in the segregation zone
CO	carbon monoxide	X_m	volumetric fraction of the conductive phase
XRD	X-Ray diffractometry	X_c	threshold concentration
SEM	scanning electron microscopy	R_m	radius of the conductive particle in the direction of electric field
CTE (α)	coefficient of thermal expansion	R_d	radius of the dielectric particle in the direction of electric field
TCR (α_T)	thermal coefficient of resistivity	t	critical exponent
T	temperature	t_F	fractal dimension in the area of conductor
E	Young modulus	g_m	array factor
K_{Ic}	fracture toughness		
LR	low resistivity		
HR	high resistivity		
IPD	insulating interparticle distance		
H	size of ellipsoid (highness) in the direction of the current flow		

are responsible for the low values of the mechanical properties, especially the flexural strength.

The properties of composites can be roughly divided into two categories: the properties which can be predicted from the properties of constituent phases, and those which cannot.⁷ To the first category can be assigned such properties as the electrical conductivity, Young's modulus, thermal expansion and hardness and to the second — flexural strength, fracture toughness and others. The addition of the second phase reinforcement can also allow retention or improvement of the mechanical properties of the matrix at room or higher temperatures, without loss of the essential physical property advantages. The maximum toughening effect of the secondary phase in CMC materials is reached with additions of between 10 and 30 vol.%, while for electrical conductivity the minimum amount of the dispersions required ranges from 20 to 30 vol.%, depending on powder particle size and the chemical composition of the matrix. Among the potential filling phases, carbides, borides, and nitrides of the transition elements (Ti, Zr, Ta) have received considerable attention. They are characterised by many outstanding physical and chemical properties and are of great interest in technology and science. The major drawback of introducing a metallic like phase in a ceramic matrix is the lower refractoriness of the composite which could preclude the use of these materials in high-temperature applications.

The need for improvement in the mechanical reliability and resistivity of two-phase electroconductive composites based on oxygen-free ceramics requires a

new approach in the development of the microstructure of CMC's and improvement in the preparation process of the raw material mixture and optimisation of the sintering step. The analysis of microstructural networks shows two typical patterns: array and random type structure (Fig. 1).⁸ The morphology, distribution and size of conducting particles for both structural patterns in two-phase composite depends on the purity and dispersion of the initial powder and on the temperature and environment of the sintering process. Fluctuation in the sintering behaviour influences the structural pattern evolution. It was already proved that the formation of the array structure in the case of the Si₃N₄–MoSi₂ composite lowers the electrical resistivity of the composite and improves the thermal resistivity coefficient.⁹ The degree of these properties evolution is strongly affected by the structural pattern or by the type of the chemical agent added.^{10,11}

The electroconductive composites of the systems: Al₂O₃–TiN, Si₃N₄–TiN, Si₃N₄–Ti(C,N) have been mainly investigated up to now.^{12–15} However, there is little data available about sintering and properties of electroconductive composites of the system Si₃N₄–TaN. Tantalum nitride is considered as a candidate for making electroconductive materials as it is characterised by many outstanding properties such as high melting point, high hardness and good electrical conductivity, and is more resistive to oxidation than TiN.¹⁶ The thermal linear coefficient of TaN is very close to that of silicon nitride which excludes in advance any thermal mismatch between the two of them in ceramic composites used at

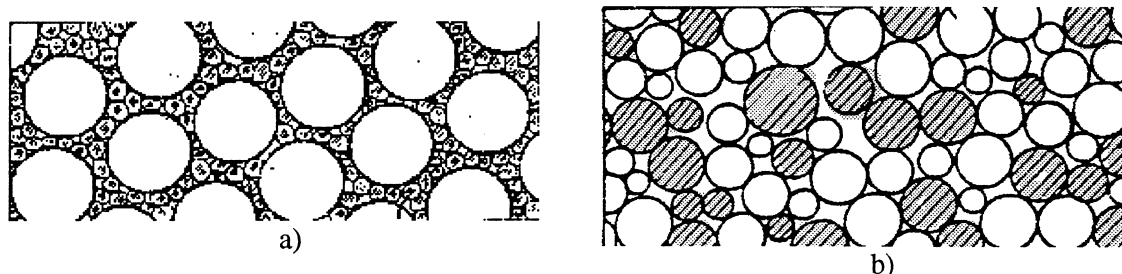


Fig. 1. Two patterns of the microstructural network: (a) array structure and (b) random structure; white-insulator agglomerates (pellets), shaded area — metal-like ceramic particles [8].

high temperatures. An overview of some physical properties of TaN and selected non-oxides are presented in Table 1.^{17–20}

All studied nitrides have a positive temperature coefficient of resistivity and often show a linear increase of resistivity up to very high temperatures. They are characterised by a wide range of possible compositions and a tendency to deviate from stoichiometry. Nitrides of transition metals are characterised by high melting temperatures, however their applications at high temperatures is limited because the nitrides have a greater tendency to dissociate than do the corresponding oxides, carbides and borides, with the exception of BN, Si₃N₄ and TaN. Therefore, these three compounds were selected for the investigation on a ceramic composite material to be used in a high temperature application (as heating elements).

The goal of this work was a systematic investigation of the sintering behaviour, microstructure, and electrical and mechanical properties of Si₃N₄–TaN composites. Due to the fact that the development of their microstructure is strongly influenced by the processing route and chemical interaction of constituents during the sintering process, the TaN powder was used in three different grain size distribution options. Two different hot pressing environments were applied in the performed experiments. The measured properties were related to the grain size of the dispersoid used and to the configuration of the conducting area in the functionally graded composites.

2. Experimental

2.1. Materials and methods

The following powders were used as the starting raw materials in the performed experiments: silicon nitride, β-Si₃N₄¹ and α-Si₃N₄,² tantalum nitride TaN + Ta₂N³

(coarse) and TaN² (fine); and alumina powder.⁴ The β-Si₃N₄ powder contained app. 12 wt.% contamination of Si₂ON₂ phase. The α-Si₃N₄ contained app. 15 wt.% of β phase. The fine TaN powder was a single phase powder and the coarse tantalum nitride powder contained app. 15 wt.% Ta₂N phase.

Size reduction of the coarse TaN powder was done by a roll milling technique.⁵ Homogenization of the powders mixture was done by a water ball milling method using alumina lining and alumina balls for 18 h (*process A*), in a planetary mixer with silicon nitride lining, made by Fritsch, for 40 min (*process B*) and in a ball-mill with alumina milling balls in acetone for 96 h (*process C*).

Green samples for the hot pressing were manufactured by tape rolling of the ceramic granulate. The extruded tape was 30 mm in width and with a thickness between 0.5 and 2.7 mm.⁵ A mixture of carboxymethyl cellulose, natural and synthetic rubber and butyral resin in quantities between 4 and 10 wt.% was used as a binder. The method of the rolling technology is described in detail in.²¹ The shaped follies were characterised by a relative density of between 54 and 75%, depending on the manufacturing parameters (number of revolutions of the roller and the thickness of tape). The green tape made from the conductive material was cut into two types of samples: samples with sizes of 15.0×15.0 mm² for the three-dimensional objects and samples with sizes of 75.0×1.5 mm² for a conducting part of the functional graded object. The green tape made from the insulating material (only Si₃N₄-based) was cut into pieces of 8.0×100.0 mm² with recesses where the samples from the conductive material were embedded (Fig. 2).²² The insulating/conductive pieces were stacked to a thickness of 10–15 mm and then uniaxially pressed. The predensified samples were sintered in a hot-press furnace in a graphite mould:

- at 1700°C for 40 min under a pressure of 20 MPa in a reducing (CO) atmosphere (due to graphite die burning),⁶

¹ Powder Metallurgy Plant, Baku, Azerbaijan.

² H.C. Starck Inc., Germany.

³ Chemical Plant, Donetsk, Ukraine.

⁴ Aluminous Plant, Nikolayew, Ukraine.

⁵ INTEM Ltd, Kiev, Ukraine, home-made rolling device.

⁶ INTEM Ltd, Kiev, Ukraine, home-made hot pressing installation.

Table 1

Selected properties of some metals and nitrides, carbides and borides which display metal-like conduction

Material	Density, g/cm ³	Thermal conductivity, W/mK	Linear expansion factor ($\times 10^{-6}$), K ⁻¹	Electrical resistivity, ρ , $\Omega \bullet \text{cm}$	Resistive temperature coeff. ($\times 10^{-4}$), K ⁻¹
Cu	8.96	400	16.5	0.17×10^{-5}	–
Ta	16.6	150	3.6	1.3×10^{-5}	400
Si ₃ N ₄	3.19	9–122	3.2	10^{13}	–
TiN	5.43	10–26	8.9	2.07×10^{-4}	600–3000
TaN	14.36	8.5	3.5	13.5×10^{-3}	900–14000
ZrN	7.35	20.5	7.3	1.4×10^{-4}	400
TiC	4.91	36.4	7.74	7.4×10^{-4}	800–9000
TaC	14.4	22.2	6.5	3.0×10^{-4}	540–3400
ZrC	6.66	41.9	6.7	7.0×10^{-4}	670–3400
TiB ₂	4.52	64.5	5.2	9×10^{-5}	300–1000
TaB ₂	12.62	16.1	8.8	3.25×10^{-4}	350
ZrB ₂	6.1	58.0	6.5	2.2×10^{-4}	250–350

- at 1740°C for 50 min under a pressure of 30 MPa in a nitrogen atmosphere.⁷

The density of sintered samples was measured by the water immersion technique. Theoretical values of 3.985 g/cm³ for alumina, 3.186 g/cm³ for silicon nitride and 14.360 g/cm³ for TaN were taken to calculate the density of the composites. The theoretical value of each composite density was calculated with the rule of mixtures assuming that no reaction takes place between the matrix material and the second phase (but sometimes this was not true).

The powder size distribution of both the starting powders and the mixtures of powders was measured in laser particle size devices: Analyzette-22 (Germany) and Powder Laser-Particles Sizer (Japan). The microstructure was observed using optical microscopy and SEM on polished and fractured surfaces of the composites. The quantitative composition of the sintered composition was determined by an image quantitative analysis technique in a SIAMS device (Russia). For the conductive phase was determined: space between conductive particles (R_d), their average size (R_m), as well as other parameters such as volume content (X_{eff}) and fractal dimension (t_F) of the area and length of the conducting phase particles. All calculations were executed between 0 and 360 degrees to the direction of the hot pressing axis. X-Ray diffraction was used to characterise the phase composition.

Electrical resistivity (ρ) was measured by a two-electrode method for both types of samples. The three-dimensional samples for the electrical properties measurement were cut at an angle of 0 and 90° to the axis of hot pressing and were of sizes $1.3 \times 1.3 \times 0.5$ cm³. The direction of measurement was always perpendicular to the hot pressing axis for the functionally graded composites (Fig. 2). The temperature dependence of the

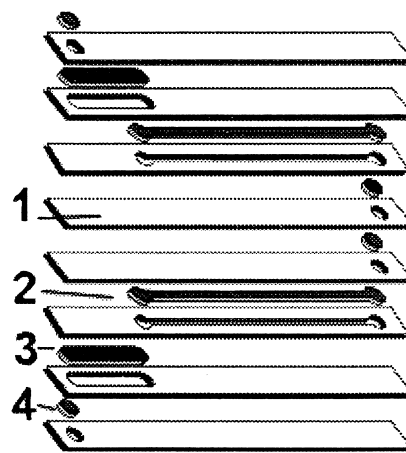


Fig. 2. A sketch of the functionally graded heating element: 1 — insulator (basic body), 2–4 — conductive heating parts.

resistivity was investigated by applying two methods: by heating in a furnace (for both types of samples) and by direct resistance heating (for FGC). The increase in temperature during the measurements was up to 4°C/min. The current density (in the latter case) was below 1.0–2.5 A/mm² at higher temperatures. At room temperature all measurements were made with a current density of app. 35 mA/mm². The temperature on the surface of FGC (in the case of the direct resistance heating) was always higher, approximately 30–50°C above the temperature of the composite body, due to the distribution of heat from the heating wires (Fig. 2, part 2).

The mechanical properties were measured on samples of sizes $6 \times 6 \times 60$ mm³ by a four-point bending test (outer span-40 mm, inner span-20 mm) with the crack plane parallel to the hot-press direction and a cross-head speed of 0.5 mm/min at room temperature. A minimum of 10 samples was used to determine the value of bending strength. The fracture toughness (K_{Ic}) was measured by the indentation method. For calculation of

⁷ FCT GmbH, Rödental, Germany.

K_{Ic} by the indentation test, the cracks induced by a Vickers pyramid under a load of 98 N were measured and the Niihara formula applied.²³ The Young's modulus (E) was measured on bars by the frequency resonance method. The thermal expansion coefficient (α) was measured using a Netsch dilatometer in the temperature range of 20–1000°C with a rate of 5°C/min.

2.2. Grain size distribution of TaN powders

In first experiments the TaN powder was used just as received from the producer (Table 2). The presence of the large particles, approx. 3–4 μm , was observed in it during the SEM investigation (Fig. 3b). The morphology and the typical grain size of the coarse TaN powder after roll milling treatment is showed in Fig. 3c. Aggregates in the range of 50–300 μm were observed in the

mixture marked BC after the homogenization process. In the case of the mixture based on the fine $\alpha\text{-Si}_3\text{N}_4$ and fine TaN powders (coded AF) ball-milled with alumina balls in acetone for 96 h (process C) only the large aggregates of approx 300 μm were observed (Fig. 4). Therefore, an adjustment in the powder grain size distribution has been done by milling the prepared composition in a ball-mill with alumina lining and alumina balls for 18 h (process A).

3. Results and discussion

3.1. Densification

All hot-pressed composites were fully dense, within the range of 97–100% of the theoretical density.

Table 2

Powder size distribution of some ceramic powders before and after homogenization process

Material (powders)	Treatment	Powder size distribution, %				
		< 1 μm	1–7 μm	7–12 μm	12–40 μm	> 40 μm
$\beta\text{-Si}_3\text{N}_4$	No	9.8	28.2	15.9	11.9	21.2
Mixture by procedure ^a	A	9.7	37.7	14.9	35.7	2.0
	B	20.3	56.7	14.1	8.9	0.0
	C	22.9	67.4	9.2	0.5	0.0
$\alpha\text{-Si}_3\text{N}_4$	No	1.9	72.2	20.4	6.5	0.0
Mixture by procedure ^b	B	26.9	55.1	10.7	7.3	0.0
TaN + Ta ₂ N (coarse)	No	1.5	17.9	28.3	45.8	6.5
	Rolled	5.5	48.4	26.3	19.5	0.3
TaN (fine)	No	1.9	72.2	20.4	6.5	0.0

^a Mixture (BC) of powders is based on $\beta\text{-Si}_3\text{N}_4$ and contains 13.5 wt.% TaN + Ta₂N (coarse) and 7 wt.% Al₂O₃ as a sintering additive.

^b Mixture (AF) of powders is based on $\alpha\text{-Si}_3\text{N}_4$ and contains 18 wt.% TaN (fine) and 7 wt.% Al₂O₃ as a sintering additive.

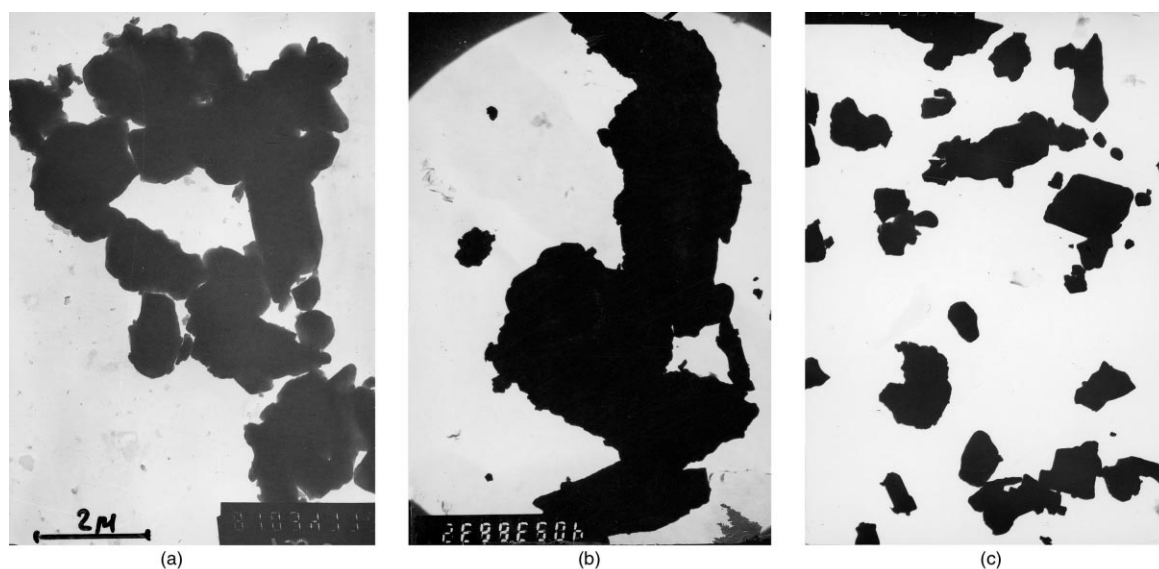


Fig. 3. SEM micrographs of the ceramic particles: (a) $\beta\text{-Si}_3\text{N}_4$ powder (mixture BC), (b) TaN + Ta₂N powder (coarse, as received), (c) TaN + Ta₂N (coarse, after roll milling treatment). Magnif.—8100x.

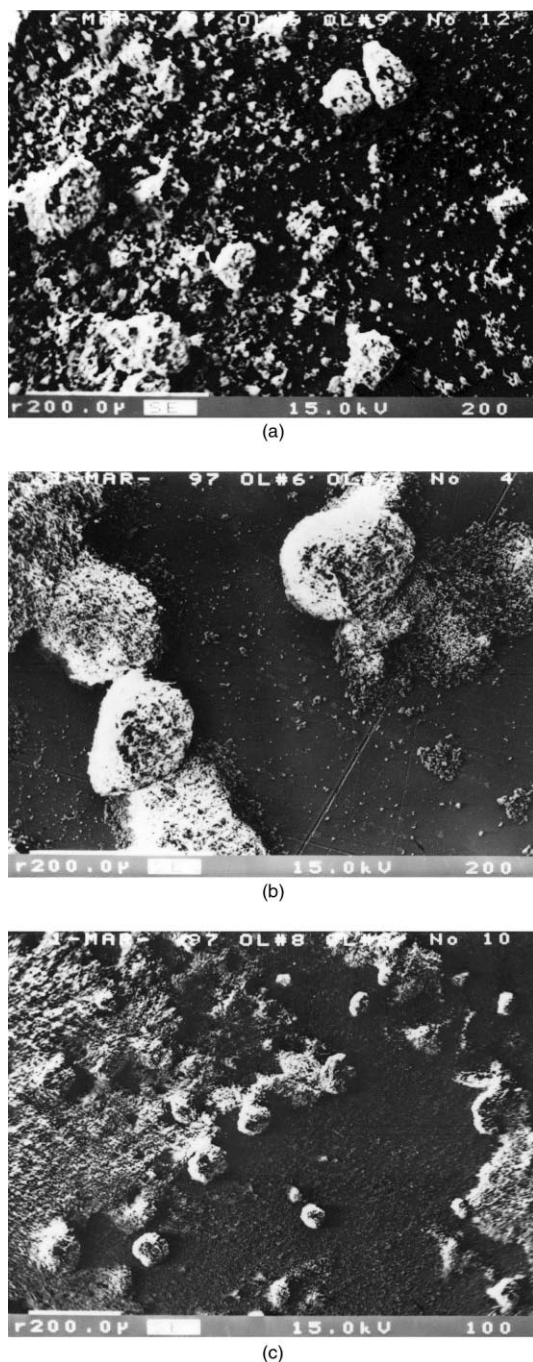


Fig. 4. SEM micrographs of the ceramic mixtures: (a) mixture BC, (b) AF after treatment by procedure B, and (c) mixture BC after treatment by procedure A. Image area: $1000 \times 700 \mu\text{m}$.

3.2. Variation in the mineralogical composition of the Si_3N_4 -TaN composite

Early work on the insulating materials in the system $\beta\text{-Si}_3\text{N}_4\text{-Si}_2\text{ON}_2\text{-Al}_2\text{O}_3\text{-TiO}_2$ proved that a liquid phase is formed in samples hot pressed in the temperature range of $1400\text{--}1700^\circ\text{C}$ in a reducing atmosphere.²⁴ It was already proved that the incorporation of O'-sialons into the $\beta\text{-Si}_3\text{N}_4$ phase gives a possibility of improving

the electrical and thermal properties of the insulating ceramics. However, an interaction between Si_3N_4 and TaN takes place during the hot pressing treatment.²⁵ Such interaction initialises a coarsening mechanism and a further evolution of the microstructure of TaN. It was already reported by Ziegler that if the quantity of a liquid phase increases without any composition changes, then the aspect ratio of the ceramic grains also increases.²⁶ If the viscosity of the liquid phase decreases without any content changes, the aspect ratio decreases. Therefore, a better understanding of the reaction sequence and densification process for the $\beta\text{-Si}_3\text{N}_4\text{-Si}_2\text{ON}_2\text{-TaN}$ composites was one of the subjects of this study.

Investigations of the phase composition of the $\text{Si}_3\text{N}_4\text{-TaN}$ composites by XRD showed that the mineralogical composition of the material strongly depended on the atmosphere of hot pressing and the quality and quantity of silicon nitride and tantalum nitride powders used. The reducing atmosphere inside the composite body is formed as a result of the pyrolysis process of organic additives inside the composite and also due to a direct contact of the ceramic material with the material of the hot-pressing mould, graphite. All reactions that take part in the composite material could be divided into 4 groups:

- (A) reactions between the gaseous environment and the two major components, Si_3N_4 and TaN,
- (B) reactions between the organic additives and the gaseous environment,
- (C) reactions between the gaseous environment and the sintering additive,
- (D) and reactions between the ceramic matrix and the gaseous inclusions.

The following chemical reactions are suggested to explain the formation of new compounds in the system $\text{Si}_3\text{N}_4\text{-TaN-Al}_2\text{O}_3$ (Table 3).

3.2.1. Mineralogical composition of the CMC material sintered in the CO environment

The mineralogical composition of the electroconductive agglomerates was measured and the results are presented in Table 4. It was observed that there was a significant growth in the volume content of the electroconductive phase when the CO atmosphere and coarse TaN + Ta_2N powder were used together. A big difference in the quantity of the resulting electroconductive phase and the quantity of introduced coarse TaN powder in the CMC hot-pressed in the reducing conditions was due to the formation of SiC and new tantalum-based electroconductive phases, products of reaction between the ceramic matrix, tantalum nitride powder, by-products from the pyrolysis of organic additives and the surrounding environment. Therefore it is suggested that a number of heterocatalytic reactions on the surface of electroconductive TaN particles took

Table 3
Typical chemical reactions which take place during the hot-pressing process in the silicon nitride-tantalum nitride composite

	Chemical reactions	Atm.
A	$18\text{TaN} + 4\text{Si}_3\text{N}_4 + \text{SiO}_2 + \text{C} \rightarrow \text{TaSi}_2 + \text{Ta}_5\text{Si}_3$ $+ 2\text{TaC}_{0.5}\text{Si} + 2\text{Ta}_5\text{Si}_3\text{N}_7 + 2\text{N}_2\text{O} + 8\text{N}_2$	N_2
	$8\text{TaN} + 3\text{Si}_3\text{N}_4 + \text{SiO}_2 + 4\text{C} \rightarrow \text{TaSi}_2 + \text{Ta}_5\text{Si}_3$ $+ 2\text{TaC}_{0.5}\text{Si} + 3\text{SiC} + 2\text{N}_2\text{O} + 8\text{N}_2$	CO
B	Natural/synthetic rubber	CO, N_2
	$[-\text{CH}_2\text{C}(\text{CH}_3)=\text{CHCH}_2-]_n \rightarrow \text{C} + \text{H}_2$	
	Butyral resine	
	$[0.7 \times (\text{C}_8\text{O}_2\text{H}_{14}) + 0.3 \times (\text{C}_4\text{O}_5\text{H}_{19})] \rightarrow \text{C} + \text{H}_2$	CO
	$\text{H}_2 + \text{O}_2 \rightarrow \text{H}_2\text{O}$	CO
	$\text{H}_2 + 3/2\text{N}_2 \rightarrow \text{NH}_3$	N_2
C	Oxidation of hot-pressing graphite die	CO
	$2\text{C} + \text{O}_2 \rightarrow 2\text{CO}; 2\text{CO} \rightarrow \text{C} + \text{CO}_2$	
	$\text{Al}_2\text{O}_3 + \text{NH}_3 \rightarrow \text{AlN} + \text{H}_2\text{O}$	CO, N_2
	$\text{AlN} + \text{SiO}_2 \rightarrow \text{SiAlO}_2\text{O}$	
	$\text{SiC} + 1/2\text{O}_2 \rightarrow \text{SiO} + \text{CO}$	
	$\text{SiC} + \text{Al}_2\text{O}_3 \rightarrow \text{Al}_2\text{O} + \text{CO} + \text{SiO}$ $\times \text{SiC} + (1-x)\text{Me} \rightarrow \text{Me}_{(1-x)}\text{Si}_x + x\text{C}$, where Me: Fe, Ni, Cr $\text{SiO}_2 + \text{O}_2 \rightarrow 2\text{SiO}$	
D	$\text{Si}_3\text{N}_4 + \text{H}_2\text{O} \rightarrow \text{SiO}_2 + \text{NH}_3$	CO, N_2
	$\text{Si}_3\text{N}_4 + \text{SiO}_2 \rightarrow 2\text{Si}_2\text{ON}_2$	CO, N_2
	$\text{Si}_3\text{N}_4 + \text{CO} \rightarrow \text{Si}_2\text{ON}_2 + \text{SiC} + \text{N}_2 (< 1820\text{K})$	CO
	$\text{Si}_2\text{ON}_2 + \text{CO} \rightarrow \text{SiO} + \text{SiC} + \text{N}_2 (> 1820\text{K})$	CO
	$2-z/2\text{Si}_3\text{N}_4 + z/2\text{AlN} + z/2$	CO, N_2
	$\text{SiAlO}_2\text{NSi}_{6-z}\text{Al}_z\text{O}_z\text{N}_{8-z}$	

Table 4
Measured content of electroconductive phases (TaN and others) in the Si_3N_4 -TaN composites

TaN in the mixture, vol. %	Content of conducting phases in the CMC by quantitative image analysis, vol. %	
	Coarse TaN additive	Fine TaN additive
<i>Hot-pressing in CO environment</i>		
10	23.9	12
13.5	24.6	
15		16
20		
25	36.3	24
40		34
50	59	
<i>Hot-pressing in N₂ environment</i>		
9	9.6	6.2
13.5	14.5	
15	15.2	—
18		12.6
25	26.9	—
40	43.3	32.3

place between the grains of TaN, Si_3N_4 and the surrounding gases (CO or N_2). It is worth noting that the presence of Ta_2N contamination in the starting coarse tantalum nitride powder stimulates the quantity of SiC

formed from the organic binder pyrolysis and the surrounding gases; approximately 10–12 vol.% in all tested samples. The SiC phase formed a network of “bridges” between the TaN grains. Other conducting phases formed during hot-pressing in the reducing condition were tantalum carbosilicide, $\text{Ta}_5\text{C}_x\text{Si}_y$, tantalum silicide, Ta_5Si_3 , and tantalum disilicide, TaSi_2 . Amounts of these silicides were measured and are related to the starting content of TaN used for the manufacture of these composites (see Fig. 5). Two types of intergranular liquids were formed in the Si_3N_4 -TaN composites during the sintering process. On the one hand the roll milling process was a source of impurities formed on the surface or inside the composite green body. The impurities promoted an interaction between the matrix and the second phase at the higher temperatures and a silicides mixture ($\text{FeSi} + \text{FeSi}_2$) was formed. The intergranular liquid phase was already formed during hot pressing at such low temperatures as 930–1230°C and the formation of this liquid promoted (acting as a catalyst) the coarsening of TaN particles (Fig. 6). Also the intergranular phase, O'-sialon based, was formed during the sintering process at temperatures above 1430–1600°C. The viscosity of this liquid decreases with the increasing temperature.¹⁵

The powder mixture containing 13% TaN was characterized by a different behaviour at the high temperatures. It is shown in Fig. 7 that most of the O' phase is exhausted at these temperatures and the β' sialon ($\text{Si}_{6-z}\text{Al}_z\text{O}_z\text{N}_{8-z}$, where $z=0.5$) is formed in small quantities as an intergranular liquid. In this case the measured resistivity of specimens was very high, approximately $5 \cdot 10^6$ ohm.cm. The formation of a big amount of the intergranular liquid, the O'-sialon and β - Si_3N_4 crystal phases was observed and the specimens were characterised by a low resistivity value, $8 \cdot 10^{-2}$ ohm.cm.

3.2.2. Mineralogical composition of the CMC sintered in the N_2 environment

The samples hot-pressed in a nitrogen atmosphere contained a lot of tantalum silicide nitride phase, only small quantities of aluminium nitride politype 27 R-AlN (approx. 4%) and $\text{Ta}_5\text{Si}_3\text{N}_7$ and traces of tantalum disilicide, TaSi_2 . The formation of SiC was negligible (Fig. 8). In this case the β - Si_3N_4 crystals are a major matrix component and the sintering process proceeds without any intergranular liquid phase forming.

3.3. Microstructure

The fracture of the insulating and conductive composites was investigated with SEM and this confirmed a fair quantity of O'-sialon in both of them, which suggested a typical sintering mechanism with the presence of a liquid phase (Fig. 9c, d). In this case, the densification,

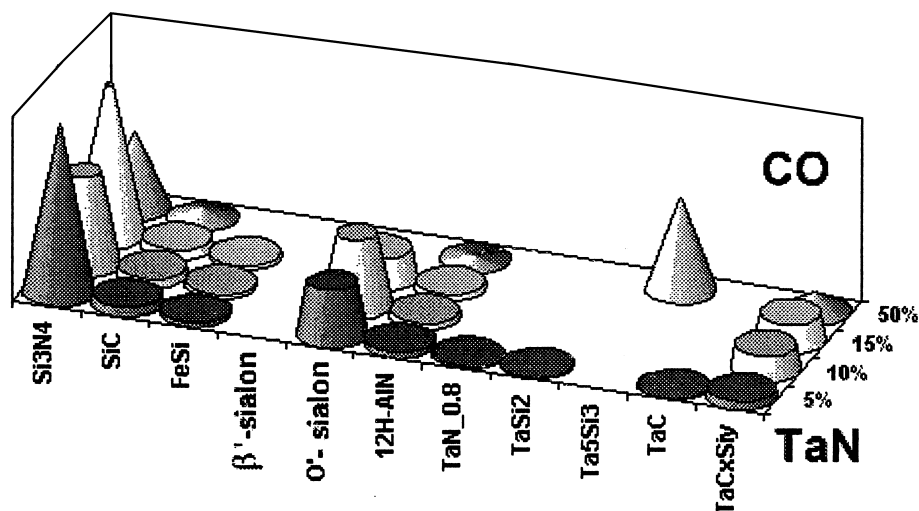


Fig. 5. Influence of the O'-sialon intergranular liquid phase on the mineralogical composition of Si_3N_4 -TaN composites: HR — a small amount of the liquid phase — high level of resistivity; LR — a high amount of the liquid phase — low level of resistivity.

contact flattening, neck growth, and microstructural coarsening (grain growth) predominantly depends on the rate of mass transfers through the liquid surrounding the solid grains during the intermediate stage of sintering. The solid phase is dissolved in the liquid phase and then the solution-precipitation phenomenon takes place. Beside the solution — precipitation process also the coalescence of small grains with contacting large grains contributes to the grain coarsening and final shape accommodation. This process is very important for achievement of the designed resistivity value of the conducting composite.²⁶

3.3.1. Influence of the grain size distribution and chemical interactions in the insulating phase on the evolution of the microstructure

The final size distribution of the conducting grains in the CMC samples based on the coarse, roll milled and fine TaN powders sintered in the N_2 atmosphere are shown in Fig. 10. The microstructure of the composites based on the β - Si_3N_4 powder are in Fig. 10a and c and based on the α - Si_3N_4 powder in Fig. 10b and d. If the coarse TaN powder with a broad grain distribution was used then the β' -sialon in the insulating phase was formed after the sintering process and the strong coarsening process of ceramic particles was observed. In the case of the roll milled TaN powder with a narrow size distribution the β - Si_3N_4 phase was formed during sintering process. The poor coarsening phenomenon and strong segregation of conducting particles in the sintering bodies were observed (Fig. 10c). In the case of the conductive ceramics with fine or roll milled TaN powders the presence of $\alpha \rightarrow \beta$ - Si_3N_4 transformation in the insulating phase after sintering process was observed, parallel to the poor coarsening and poor segregation phenomenon (Fig. 10b and d). The increase in the TaN

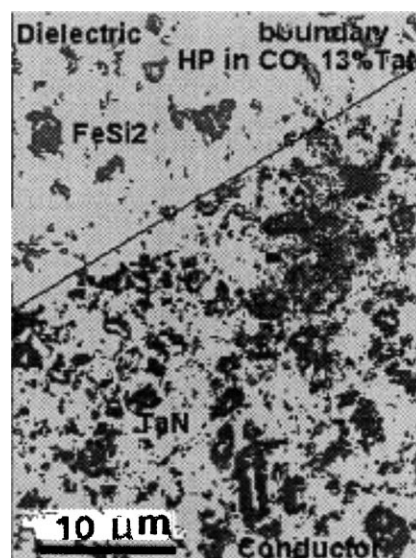


Fig. 6. Influence of iron disilicide on the coarsening of TaN particles in the functionally graded composite.

grain size (app. $3.5 \mu\text{m}$) and increase in their elongation ratio (1.74/1) were observed for the composites sintered in the N_2 atmosphere. The use of mechanical activation during the manufacturing process (i.e. ball milling) decreases the asymmetry of TaN in the composite to 1.44/1. This effect was even stronger when the reducing environment was applied (CO) during the sintering process. The average grain size of TaN was app. $2.25 \mu\text{m}$ and the asymmetry ratio was 1.34/1. The composite made with the fine TaN powder (from H.C. Starck) as a base was characterised by a very small volume of the electroconductive phase in the matrix, low average grain size — $1.5 \mu\text{m}$ and asymmetry of 1.47/1 (Fig. 10b).

According to the chemical reaction sequences (Table 3, C and D) between products of pyrolysis of organic

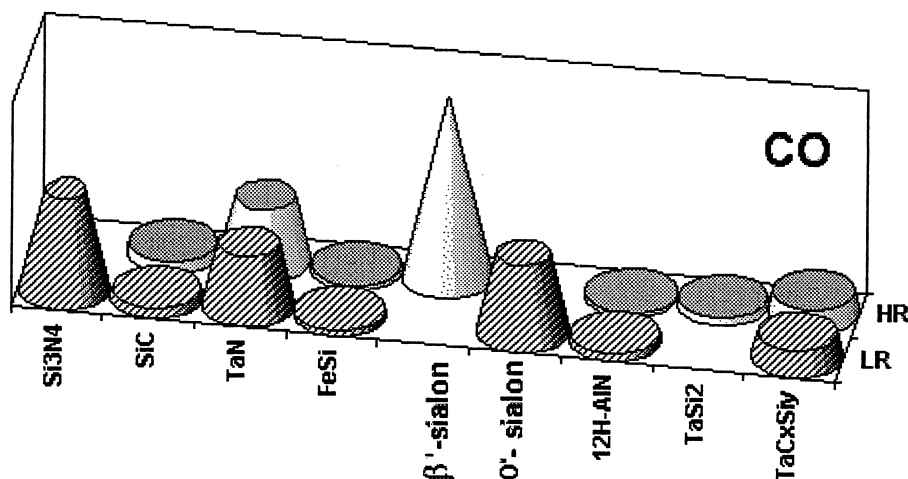


Fig. 7. Mineralogical composition of CMC hot pressed in a CO atmosphere in relation to the content of the coarse TaN powder.

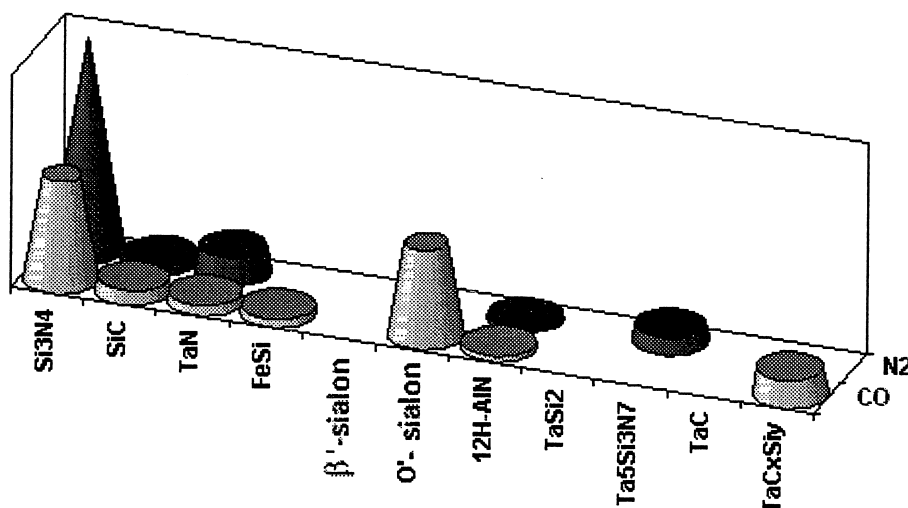


Fig. 8. Influence of the atmosphere of hot pressing on the mineralogical composition of the Si_3N_4 -TaN composite with 13% TaN: CO — reducing atmosphere, N_2 — nitrogen atmosphere.

binders and sintering additives, different AlN polytypes could be achieved. These reactions are accompanied by a microcracking phenomenon and, as a result of this, an imperfection in the microstructure of the sintered samples (Fig. 11). The defects formed in the samples sintered in the CO atmosphere were isolated from each other and differed from the defects formed in samples hot pressed in the N_2 atmosphere, which were mainly of an elongated shape. A boundary between the dielectric and the conductive phases is shown in a micrograph in Fig. 11a. The number of microcracks in the studied composite is low. The majority of pores were eliminated by the agglomeration process and the growth of coarse $\text{TaN} + \text{Ta}_2\text{N}$ grains. All pores located on the interface between dielectric and conductive agglomerates disappeared and the residual porosity was homogeneously distributed in the composite. A quite opposite situation

was observed in the composite made from the fine TaN powder and sintered in the nitrogen atmosphere. The quantity of defects on the dielectric/conductor interface was proportional to the quantity of introduced electroconductive phase. The high concentration of such defects in the composite body was also a source of microcrack formation, with cracks as long as 100 to 1000 μm (Fig. 11b). Thus, the CO atmosphere is preferred for the low-defects manufacturing process.

Compositions with the O'-sialon additive have been characterised by a different behaviour at high temperatures.²⁷ It was established that most of the O' phase is exhausted at 1700°C and the expected ratio of β'/O' -sialons cannot be obtained. The O' phase formation starts at about 1400°C and increases with the temperature increase up to about 1600°C. The β' -sialon phase then increases rapidly at the expense of non-reacted α -

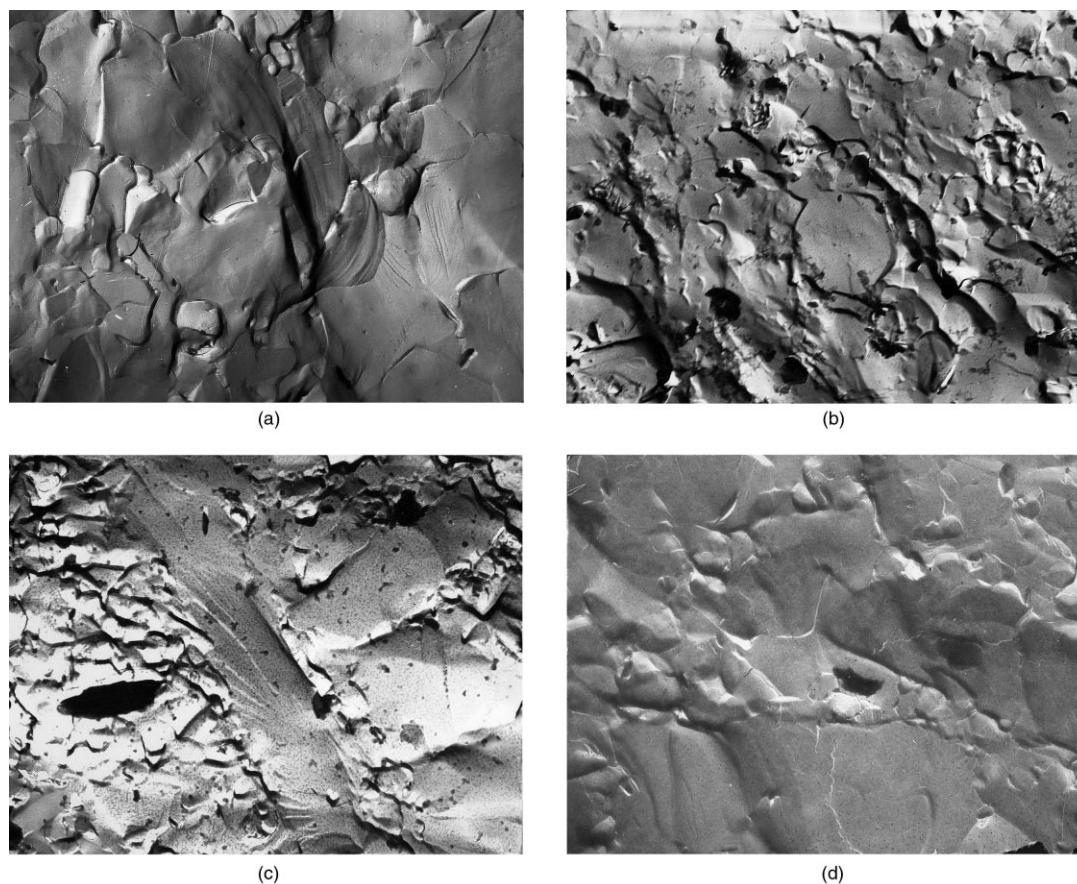


Fig. 9. SEM micrographs of fractured surfaces of the Si_3N_4 -TaN composite. The following phases are shown: (a) insulator $\beta\text{-Si}_3\text{N}_4 + \beta'\text{-sialon}$, HP in CO atmosphere; (b) insulator $\beta\text{-Si}_3\text{N}_4$, HP in N_2 atm.; (c) insulator $\beta\text{-Si}_3\text{N}_4 + \text{O}'\text{-sialon}$, HP in CO atm.; (d) conductor $\beta\text{-Si}_3\text{N}_4 + \text{O}'\text{-sialon} + \text{TaN}$, HP in CO atm.

Si_3N_4 and some O' sialons are formed in the final product. In the materials with a low level of the liquid phase the coalescence process goes ahead very slowly (Fig. 12). According to R. German a high dihedral angle, large grain size differences and a high level of liquid (about 10–30%) in the powder system contributes to the easy coalescence. The coarsening time will vary with the cube exponent of the smaller grain size.²⁸ It was estimated that the level of intergranular liquid for the samples showed in Fig. 12a and b was 20 and 5 vol.%, respectively.

3.3.2. Influence of the TaN volume fraction and geometry of the strip area on the evolution of microstructure in the monolithic and functionally graded composites

The microstructure of the composites with a content of TaN in the range of 5–50 vol.% were studied. The results are presented in Table 4 and Fig. 13. In the poorly packed compacts the coarsening process is initially not so effective in the promotion of densification because of the poor particle contacts. A small fraction (approx. 3%) of the initial grains contact will undergo a coalescence in the first minutes of the sintering process. A certain particle size distribution is probably sufficient

to initiate the evolution of network microstructure in any powder compact and also some increase in the amount of the second phase is required to facilitate the sequence of events which are shown in Fig. 13. This coarsening mechanism is beneficial for the homogenization process, but it cannot be included in the densification process.

The obtained data and performed analysis suggest that if the dihedral angle is greater than zero then the grain boundaries in the crystalline powder system are formed between grains after a relatively short sintering time. Also the connectivity and continuity increases. In the case of a low amount of the secondary phase, there will be rapid grain motion in the liquid. It is well known that during this motion the grain contacts are formed which probably promote the coalescence process. An isolated microstructure is anticipated when the time for coalescence is short in comparison to the time between the grain contacts. The isolated structure would be favoured by the low dihedral angle or rapid coalescence as compared to the contact frequency. The conductive agglomerates are shaped by a rapid coalescence as compared to the contact frequency (Fig. 14). At a certain content of the secondary phase (the threshold

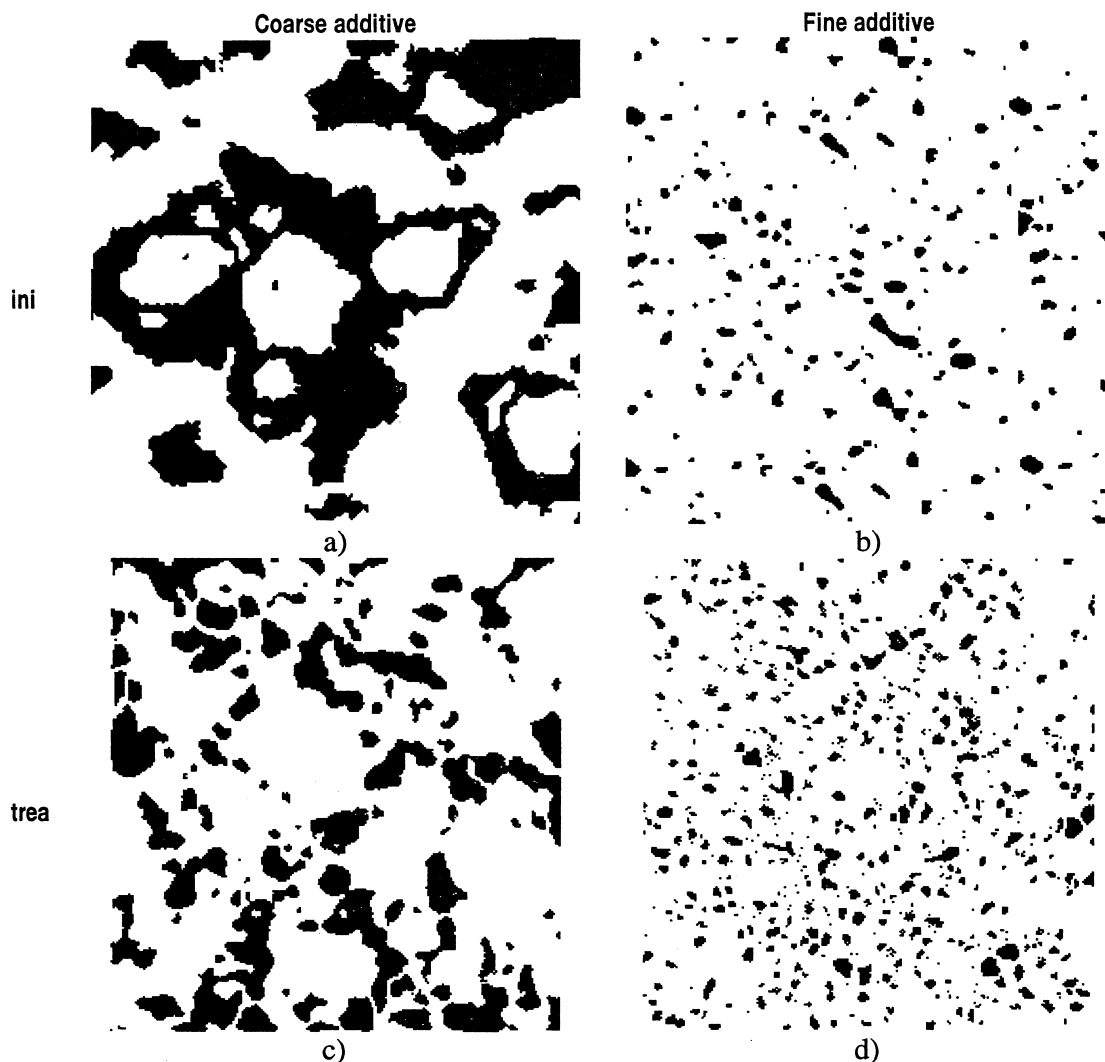


Fig. 10. Differences in the microstructure of the Si_3N_4 -TaN composite hot pressed in the N_2 atmosphere with (a) coarse, (c) segregated and (b, d) homogenized powders. The amount of TaN in mixture: a, c — 25 vol.%, b — 10 vol.% and d — 18 vol.%. Abbreviations: ini — TaN powder as received; trea — TaN powder after (c) roll milling and (d) ball milling process. Investigated area: (a–c) $61 \times 61 \mu\text{m}$; (d) $45 \times 45 \mu\text{m}$.

concentration) a skeletal structure was formed (Figs. 13a and b and 15c). This skeletal microstructure of the conductive phase is most typical for the liquid phase sintering when the coalescence time is long in comparison to the frequency of grain contacts, and there is a finite dihedral angle. Since the packing co-ordination of grains increases with the volume fraction of the solids, the probability of coalescence also increases with higher volume fraction of the solids. On the other hand, the grain motion in the liquid is inhibited by a high volume fraction of the solids. Consequently, the coalescence is estimated to be important only for the first 10 min after liquid formation for most of the systems.^{15,29}

The contribution of the linear shrinkage of each component in multiphase systems is related to the coalescence process which is very important for the microstructure development. An insulator phase in the Si_3N_4 -O'-sialon-TaN composite starts shrinking at a tempera-

ture of about 1400°C and this effect increases with the temperature up to about 1680°C . The linear shrinkage of the conducting particles starts just above 1400°C . Obviously, in this case the skeletal structure of conducting particles will be transformed into an isolated structure with a high probability that a number of the conducting grain contacts will decreased. This is confirmed by a packing model of particle coarsening suggested by Chen as is schematically illustrated in Fig. 16.³⁰ The coarsening of conducting particles under these assumptions leads to the decrease in insulating agglomerates volume and to the increase in packing density of the conductive grains. This involves a co-ordinated inward movement of particles in a “ring” towards the central insulating agglomerate and it maintains the particles in contact. As the extra agglomerate space is displaced to the exterior of the ring, a compact body composed of such particle rings shrinks macroscopically.

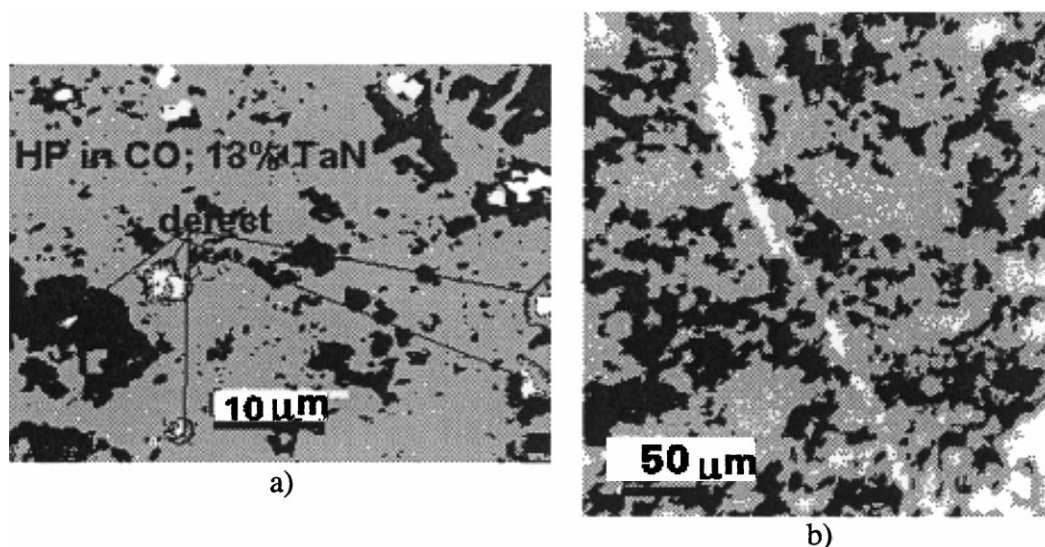


Fig. 11. Imperfection in the microstructure of CMC as a result of chemical reaction between products of pyrolysis of the organic binder and sintered additives. The sample were hot pressed in (a) CO; (b) N₂ atmosphere. White field shows a microcracking.

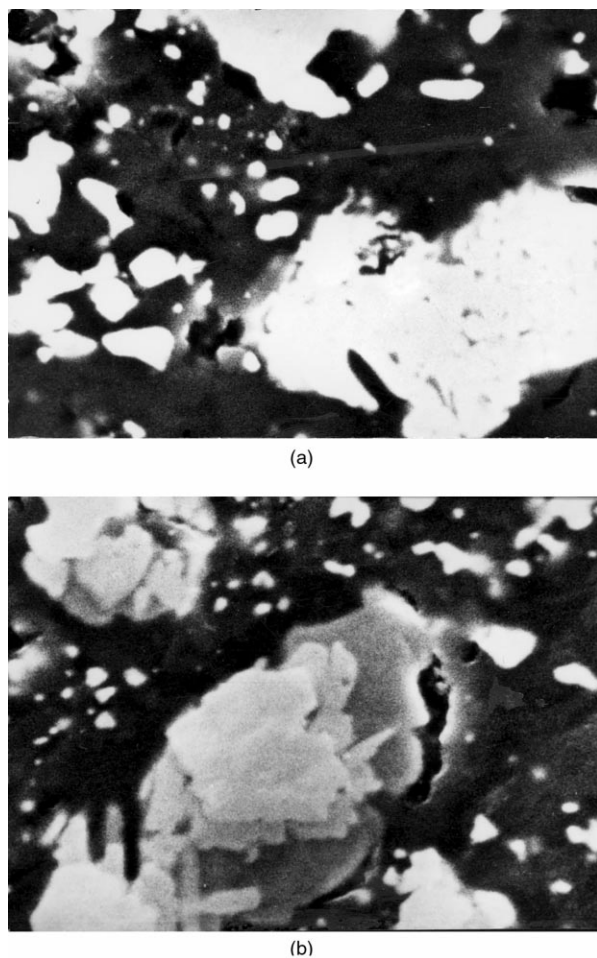


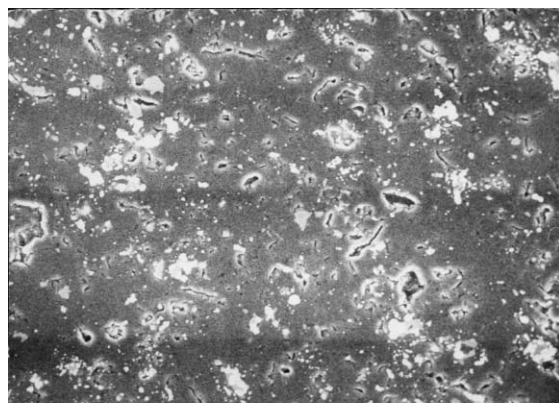
Fig. 12. SEM micrographs showing the coarsening effect and grain shape accommodation phenomenon in the Si₃N₄-O'-sialon-TaN sample sintered in the CO atmosphere: (a) high level of the intergranular liquid phase (sample with a low resistivity value), (b) low level of the intergranular liquid phase (sample with high resistivity value). Magnification — 3500x.

Then the contacts between conductive grains are broken. The capillary forces will promote the motion of grains and as a result, new contacts are formed and changes in the overall dimension of the network are promoted. This process is continued up to the moment when any further particles rearrangement is possible. It is assumed that this process would be possible in the multiphase system where an existence of few threshold concentrations for insulated-skeletal microstructural transformation are present. It was also discovered that the microstructure of the hot-pressed composite with coarse TaN particles sintered in the CO atmosphere was characterised by the presence of long chains of conductive agglomerates built-up from elongated shape basic units. These chains are preferentially orientated in the direction at 135° to the hot pressed axis. Such a type of microstructure, however, was not observed for the composites made with a fine TaN powder.

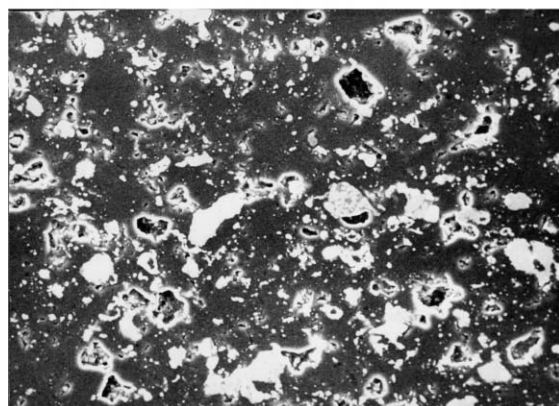
The performed studies on a correlation between the degree of grains growth and the geometry of the conducting strip area in the functionally graded material have shown that this degree is characterised by a non-linear functional dependence on the width/thickness ratio (b/t) in the strip area and the amount of the conductive phase (Fig. 17). It is obvious that for each amount of the conducting additive there exists a defined, optimal value of the b/t parameter.

3.3.3. Quantitative evaluation of the grain growth and the grain aspect ratio in the conductive CMC

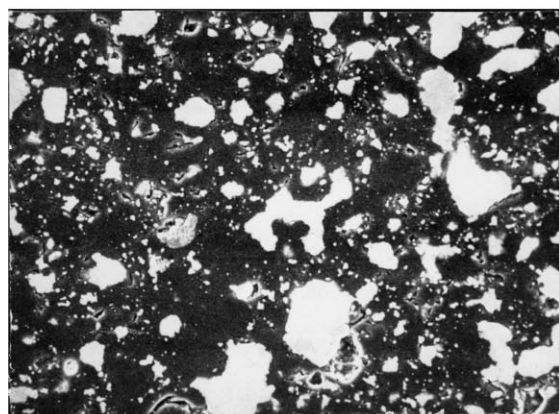
Several hundred metallographic images of different CMC fragments were studied and the results of this analysis are summarised in Figs. 13 and 15. A typical size change of the conductive agglomerates, R_m , and the insulating agglomerates, R_d , for materials with the



(a)



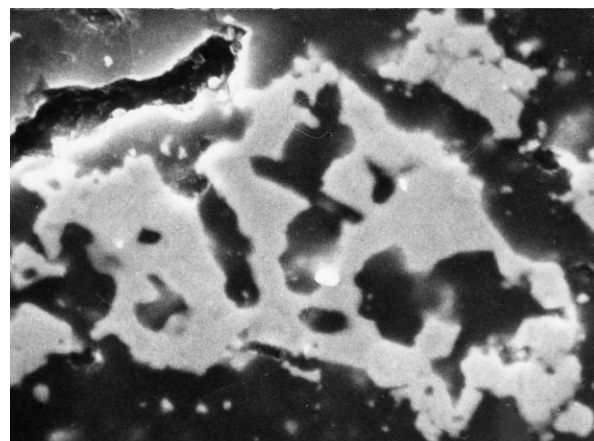
(b)



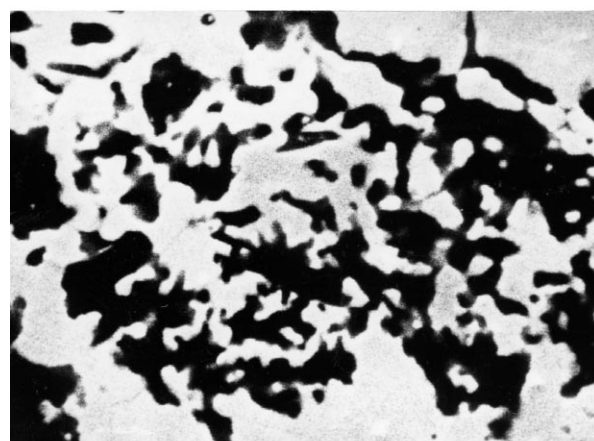
(c)

Fig. 13. Metallographic image of the monolithic sample hot pressed in the CO atmosphere. Addition of the coarse TaN powder with a large grain distribution in quantities: (a) 5 vol.%; (b) 10 vol.%; (c) 15 vol.%. The quantity of the intergranular liquid is above 15 vol.%. Magnification — 500 \times (image area — 180 \times 180 μ m).

structures shown in Figs. 12, 13 and 15 are presented in Fig. 18. Two different characteristic size changes were observed for the composites with an effective concentration in the range of 11–34 vol.%, with a low and high resistivity level. The composites with a low secondary phase content (up to 11%), prepared with roll milled powders, were characterised by low resistivity values and



(a)



(b)

Fig. 14. Shape of the conductive agglomerates (pellets) after coalescence process (close to the threshold concentration of the filling phase). Addition of the coarse TaN powder — 14.0 vol.%. The quantity of the intergranular liquid phase is above (a) 15 vol.%, (b) 5 vol.%. Magnification — 5000 \times (image area — 17 \times 17 μ m).

small sizes of the conductive agglomerates (1.0–2.5 μ m) and insulating interparticle distances (15–20 μ m). The coarsening mechanism of the conductive agglomerates in the composite with the secondary phase amount of 12 vol.% and higher was changed and a new type of structure rearrangement was observed for materials with the secondary phase content from 12 to 34 vol.%. The conductive agglomerates reached a size of 4.0–4.5 μ m; however the rate of coarsening process was much lower. The insulating interparticle distances followed the former tendency of decreasing and their values were close to 10 μ m. This phenomenon differs even much more in the composites with the secondary phase (filler) in the range of 34–50% where an anomalous decrease in the size of conductive agglomerates, from 4.5 to 3 μ m, was noticed with a further growth in their content. At the same time a more intensive decrease in the interparticle distance value from 10 to 2.5 μ m was measured. A further increase in the secondary phase content leads again to

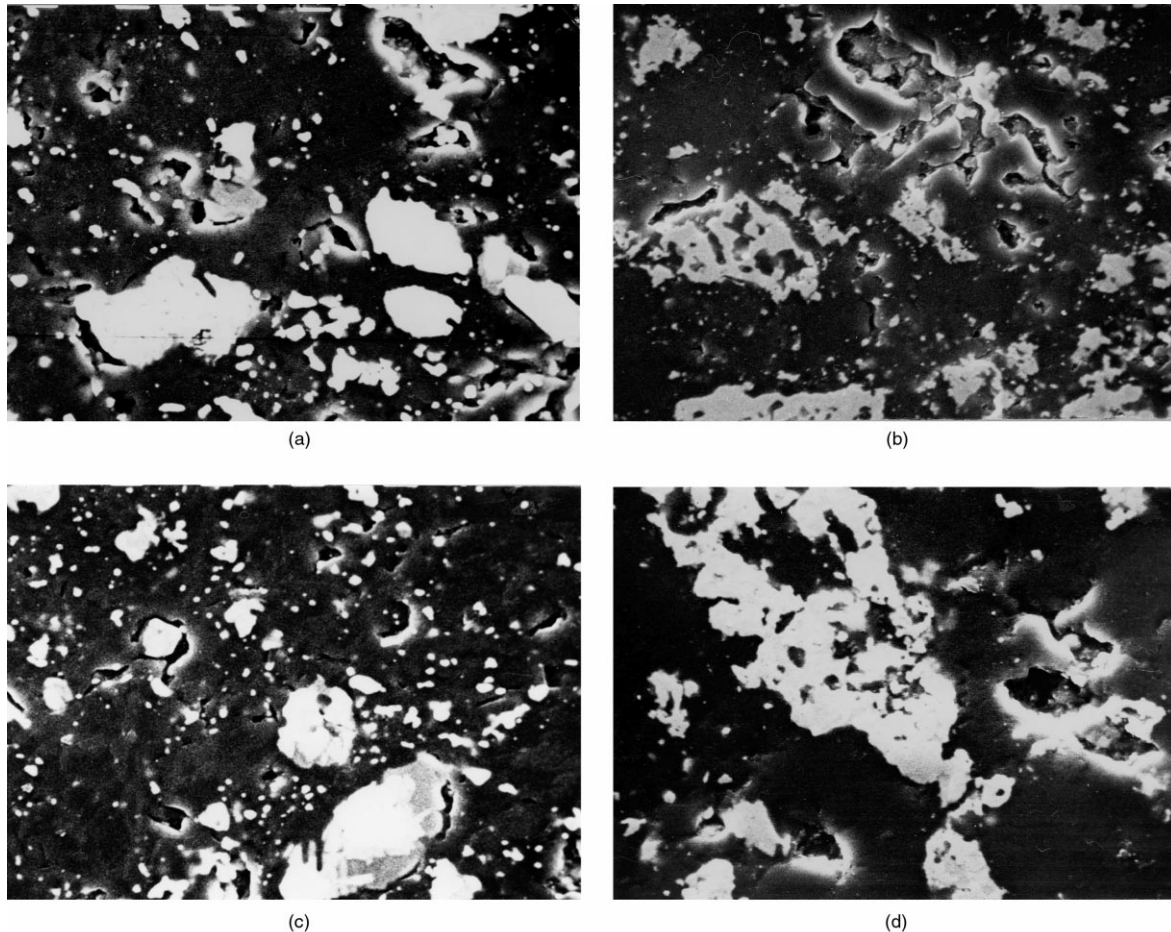


Fig. 15. Metallographic image of (a, c) the bulk composite material and (d) conductive strip area of FGM ($b/t=6$) hot pressed in the CO atmosphere. Addition of the coarse TaN powder — 14.0 vol.%. The quantity of the intergranular liquid phase of above: (a, b) — 15.0 vol.%, (c, d) — 5.0 vol.%. Image area: (a-c) $61 \times 61 \mu\text{m}$; (d) $45 \times 45 \mu\text{m}$.

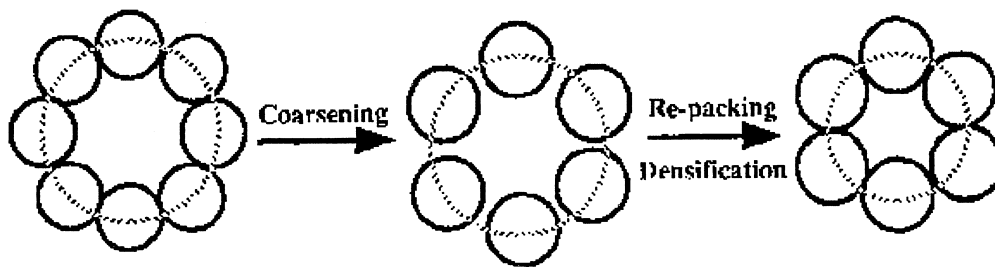


Fig. 16. A sketch of the particle coarsening process and re-packing phenomenon for a two-component powder system according to [30].

the conductive agglomerates growth and anomalous growth of the insulating interparticle distances (IPD).

Composites made on the base of coarse powders (with high resistivity level) and with a low secondary phase content were characterised by higher values of the conductive agglomerates sizes (about 2.5 μm) and as well as the insulating interparticle distances (approx. 30 μm). Dimensions of the conductive agglomerates were almost not influenced with the secondary phase growth up to 22 vol.% and then a very sharp increase was observed.

With a growth of the secondary phase content up to 7 vol.%, the conductive particles grew up 1.5 times. The IPD decreased first down to 7 μm at the content of the secondary phase of 22%, and then started growing again, up to 9–10 μm . With a further increase in the secondary phase content the change in the conductive agglomerates size and IPD were similar to those for the material with roll milled powders. The fractal of the secondary phase was defined by a method of enlarged grids. The results of performed measurements are given in Fig. 19.

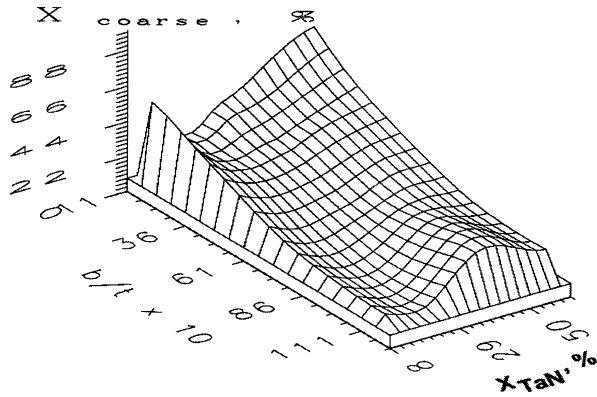


Fig. 17. Correlation between the grain growth rate and the ratio of width/thickness (b/t) in the FGM's strip area and the amount of the conductive phase in the $\text{Si}_3\text{N}_4\text{-O}'\text{-sialon-TaN}$ composite with coarse TaN powder.

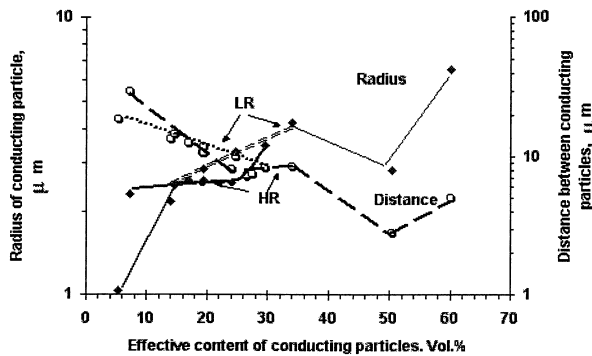


Fig. 18. Correlation between the particle size of conducting and insulating agglomerates and the effective concentration of the filler phase. LR — low resistivity CMC, HR — high resistivity CMC.

Composites made on the base of roll-milled powders with the second phase content in the range up to 11 vol.% were characterised by a constant fractal of length; in the range of 10–18% — by a fractal of conductive agglomerates area. Composites made on the base of coarse powders were characterized by an area fractal only. A specific feature of the fractal was that its value gradually increases to a value of about 0.25 with an increase in the content of conductive agglomerates to 11, 18, 32 and 50 vol.%. An estimated correlation between the aspect ratio of the conductive agglomerates and the direction of hot pressing and content of the secondary phase was also very similar (Fig. 20). Chord “H” to the direction of hot pressing at 90 and 135° angle and chord “D” in the perpendicular direction were measured to define H/D the aspect ratio of the conductive agglomerates. A high asymmetry to the direction of hot pressing axis of 135° was noted which decreases with the increase of the second phase effective content for fine powders. In the concentration range of 12–22% the conductive agglomerates made on the base

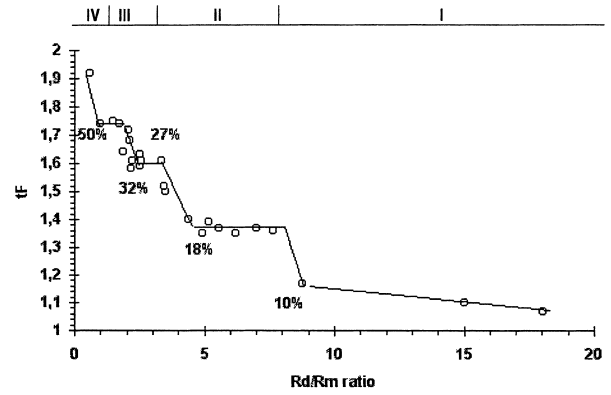


Fig. 19. Fractal for the filler phase in the two-phase CMC.

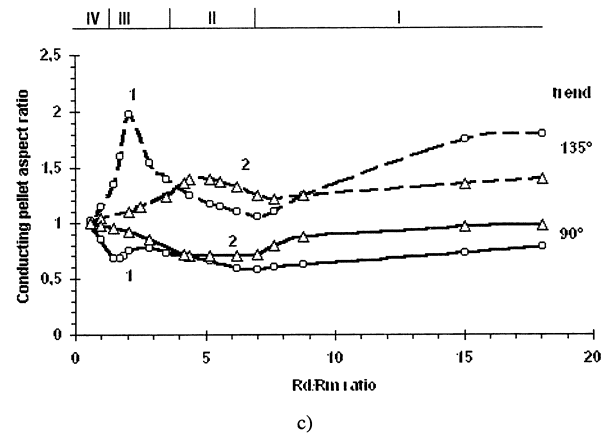


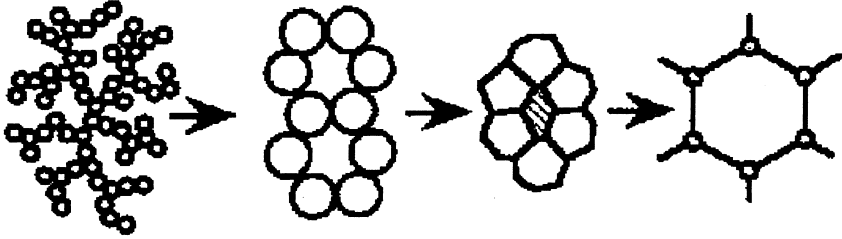
Fig. 20. Correlation between the aspect ratio of conducting pellets and the R_d/R_m ratio for (1) fine and (2) coarse particles of the filler phase. Direction to HP axis — 90° marked by a continuous curve; 135° to HP axis — dashed curve.

of fine powders were practically isometric. Then, in a concentration range of 25–40%, the fine powder forms highly elongated particles with a $H/D=1.5\text{--}2.0$ with a maximum elongation at the second phase concentration of about 33 vol.%. Anisotropic agglomerates were observed in the case of a CMC with the coarse powder used in the range of 12–25 vol.%, with a maximum anisotropy at about 18 vol.%.

Therefore, on the basis of obtained results it was concluded that for the two-phase composites the degree of structure regularity is strongly dependent on the second phase content (Table 5). In accordance with⁵ the structure regularity level can be quantitatively estimated by an array factor which is defined as a ratio of the two-phase composite interfacial surface area to the total surface area of particles of a selected phase:

$$g_m = \frac{1 - \frac{R_m}{R_d}}{1 + \left(\frac{1 - X_m}{X_m} \right) \cdot \frac{R_m}{R_d}} \quad (1)$$

Table 5
An arraying scheme for the secondary phase (filler) particles in the two phase CMC

An arraying level of conductive particles			
I	II	III	IV
			
Threshold concentration value, vol. %			
4–9.5–12.5	18–22	27–34–38	50–65
R_d/R_m Ratio			
20–9–7	5–3.5	3–1.5	< 1
2D Coordination of conducting particles/theoretical threshold concentration value, vol. %			
Triangle/0.225 ($z = 18$)		Triangle/0.295 ($z = 12$) or 0.345 ($z = 6$)	Square/0.5 honeycomb/0.65
3D Coordination of conducting particles/theoretical threshold concentration value, vol. %			
Body centre cubic/0.119 honeycomb/0.124 ($z = 12$)	Side centre cubic/0.178 ($z = 8$) simple cubic/0.247 ($z = 6$)	Diamond/0.388 ($z = 3$)	
Fractal			
< 1.1	1.35	1.6	1.9
Coordination number z			
18–12	8/6	6/3	4/3

where:

g_m — array factor,
 R_m, R_d — size of the conductive and insulating
agglomerates,
 X_m — content of the second (conductive) phase.

If the array factor is equal to 1 — the structure is considered to be arraying, if this coefficient is equal to 0 — the composite is the statistically ideal phase mixture. The arraying factor of the investigated composites was calculated from Eq. (1) and the results are presented in Fig. 21. As is shown in Fig. 21, a high arraying level of the structure is preserved for the structural level I and II (see Table 5) for the composites made from fine powders. If the coarse powder was introduced as a filler into the monolithic (bulk) composite a rapid shift to the state of the statistical mixture began in the tested samples (Fig. 21, curve 3) starting from the structural level II. For the conductive area in FGM such a shift of the system to the statistical mixture area only took place for the composite with a content of filler of about 25% which response to the structural level III.

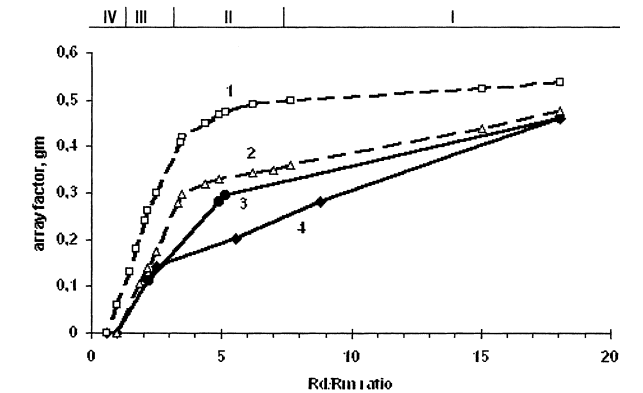


Fig. 21. The array factor for the conducting phase in the two-phase composite. Filler phase used as a (1) fine, (3) milled and (2, 4) coarse powder. Continuous curve — bulk material; dashed curve- conducting area of FGM.

4. Summary

The results of the microstructure evaluation can be summarised as follows:

- In the electroconductive Si_3N_4 -TaN composites made with the coarse TaN + Ta_2N powder, the conductive clusters consist of a mixture of TaN and by-products of the reaction between the TaN, the Si_3N_4 matrix and the surrounding gases. The use of fine, pure TaN powder results in a very low or negligible content of SiC in the sintered composite body.
- The morphology of hot-pressed Si_3N_4 -TaN composites strongly depends on the quality of ceramic powder used, grain sizes distribution and atmosphere during hot pressing.
- Agglomerates of the electroconductive phase have changed their aspect ratio during the hot-pressing process and were characterised by an elongated shape. They are oriented at an angle of lower than 135° to the hot-pressing axis.
- Electroconductive clusters formed in the hot-pressed composites are organised in a “chain” type-interconnecting network if the coarse TaN/ Ta_2N powder and reducing atmosphere were applied. The agglomerates of conducting pellets look like “laces” consisting of several monoparticles separated by the dielectric phase. The grains of electroconductive phase are surrounded by SiC nanoparticles formed during the hot-pressing process. The defects formed during the processing are homogeneously distributed in the composite.
- The composites made from the pure, fine TaN powder and hot pressed in the nitrogen atmosphere do not have any inclusions of the SiC phase. These composites consisted mainly of two phases, silicon nitride and tantalum nitride (organised in a “ring” shape network); defects are agglomerated in the microcracks and unevenly distributed in the composite body.

References

1. Gogotsi, Yu.G., Review; particulate silicon nitride-based composites. *J. Mater. Sci.*, 1994, **29**, 2541–2556.
2. Scheppokat, S., Claussen, N. and Hannick, R., RBAO composites containing TiN and TiN/TiC. *J. Eur. Ceram. Soc.*, 1996, **16**, 919–927.
3. Prakash, B., Mukerji, J. and Kalia, S., Tribological properties of Al_2O_3 -TiN composites. *Am. Ceram. Soc. Bull.*, 1998, **77**(9), 68–72.
4. Kim, W. J., Taya, M., Yamada, K. and Kamiy, N., Percolation study on electrical resistivity of SiC/ Si_3N_4 composites with segregate distribution. *J. Appl. Phys.*, 1998, **83**(5), 2593–2598.
5. Skorochod, V., Structural and percolating effects in theory of generalized conductivity of ceramics and ceramic composites. *Polish Ceramic Bulletin*, 1995, **47**(9), 39–46 (in Russian).
6. Magley, D. J., Winholtz, R. A. and Faber, K. T., Residual stress in two-phase microcracking ceramics. *J. Am. Ceram. Soc.*, 1990, **73**(6), 1641–1644.
7. Guicciardini, S., Compositional dependence of mechanical and wear properties of electroconductive ceramics. *Powder Metallurgy and Metal Ceramics*, 1999, **38**(3–4), 138–148.
8. Progogine, I. and Stengers, I., *Order out of Chaos*. London, 1984.
9. Asumi, M., Yoshida, H. and Into, N., Sintered ceramic electric heater with improved thermal shock resistance. Patent USA No 4633004 MKI H05B 3/12 from 30.05.1984.
10. Hermann, M., Baltzer, B., Schubert, Chr and Hermel, W., Densification, Microstructure and Properties Si_3N_4 -Ti(C,N) Composites. *J. Eur. Ceram. Soc.*, 1993, **12**, 287–296.
11. Peni, F., Crampon, J. and Duclos, R., The effect of TiN and TiC dispersoids on the high-temperature deformation mechanisms of Si_3N_4 . *Ceramic Int.*, 1992, **18**, 413–425.
12. Bellosi, A., Guicciardini, S. and Tampieri, A., Development and characterisation of electroconductive Si_3N_4 -TiN composites. *J. Eur. Ceram. Soc.*, 1992, **9**, 83–93.
13. Tampieri, A. and Bellosi, A., Oxidation resistance of alumina-titanium nitride and alumina-titanium carbide composites. *J. Am. Ceram. Soc.*, 1992, **75**, 1688–1690.
14. Mukerji, J. and Biswas, S. K., Synthesis, properties, and oxidation of alumina-titanium nitride composites. *J. Am. Ceram. Soc.*, 1990, **73**(1), 142–145.
15. Petrovsky, V.Ya., Use of conducting composite based on Si_3N_4 in broadband electric heaters. Part I. Fabrication of the functional element. *Powder Metallurgy and Metal Ceramic*, 1998, **37**(3–4), 174–181.
16. Petrovsky, V.Ya. and Skorochod, V. V., Physical principles and technological aspects of the production of gradient composites based on an oxygen-free ceramics. *Powder Metallurgy and Metal Ceramics*, 1999, **38**(3–4), 115–125.
17. Wang, C. C., Akbar, S. A., Chen, W. and Patton, V. D., Review; Electrical Properties of High-Temperature Oxides, Borides, Carbides, and Nitrides. *J. Mat. Sci.*, 1995, **30**, 1627–1641.
18. Winter, V., Elektrische Heizbarkeit und Mikrostrukturierbarkeit einer Mischkeramik aus Aluminiumoxid und Titanitrid, Report Fortschungszentrum Karlsruhe GmbH, no FZKA 6173, 1998.
19. Semchyshen, M. and Harwood, J. J., *Refractory Metals and Alloys*. Interscience Publishers, New York, 1961.
20. Samsonow, G.W. and Winicki, I.M., High melting compounds (Tugoplavkije sojedinenija, Sprawocznik, Metallurgija), Moskwa, 1976 (in Russian).
21. Petrovsky, V.Ya., Shaping of Ceramic Follies for O' Sialon-based Functionally Graded Composites. *Polish Ceramic Bulletin*, 1997, **54**(16), 249–258.
22. Pat. 94917644.0-2211 Europ., MKI H05B 3/14 from 09.02.1995, Keramische Heizelemente sowie Verfahren zur Herstellung eines solchen Heizelements, V.Ya. Petrovsky.
23. Birkley, I. and Stevens, R., Applications of zirconia ceramics. In *Key. Eng. Mat.*, Vols. 122–124. ed. H. Mostaghaci, 1996, pp. 527–552.
24. Petrovsky, V.Ya., The role of liquid phase in the realisation of some properties sialon-based ceramics. *Polish Ceramic Bulletin*, 1993, **45**(7), 40–50 (in Russian).
25. Petrovsky, V.Ya., Olejnik, G. and Raabe, J., Interaction of crystal phases in complex sialons. *Polish Ceramic Bulletin*, 1992, **41**(3), 45–51 (in Polish).
26. Braue, W., Wetting, G. and Ziegler, G., Role of Interface in Ceramic Microstructure '86, ed. J.A. Pask and A.G. Evans, Plenum Press, New York, 1987, pp. 883–886.
27. Petrovsky, V.Ya., Method of studying the sialon wetting with oxides of silicon, aluminium, calcium and titanium. *Key Eng. Materials*, 1994, **89-91**, 265–268.
28. German, R. M., *Liquid Phase Sintering*. Plenum Press, New York, 1985.
29. Countney, T. H., Densification and Structural Development in Liquid Phase Sintering. *Metall. Trans. A*, 1984, **15A**, 1065–1074.
30. Chen, P. L. and Chen, I.-W., Sintering of fine oxide powders, Part I: Microstructural evolution. *J. Am. Ceram. Soc.*, 1996, **79**(12), 3129–3141.